A Dynamical Game Approach for Integrated Stabilization and Path Tracking for Autonomous Vehicles

Ehsan Hashemi, Xingkang He, and Karl Henrik Johansson

***Abstract*— A new game theory based framework is proposed for path tracking and stabilization of autonomous vehicles. In the developed framework, vehicle body and corner traction control strategies are formulated in terms of players in a differential game. An integrated stability and path tracking control based on a non-cooperative differential game is developed. It includes bidirectional slip effect and wheel dynamics, which reflect more accurate longitudinal and lateral dynamics in harsh maneuvers and scenarios with sudden changes in the path planners trajectories. The open-loop and closed-loop Nash equilibrium control strategies are obtained by solving a two-player linear-quadratic differential game for the dynamical system of the overall tracking error. The performance of the proposed control strategy is validated with software simulations in various driving conditions.**

I. Introduction

Game theory is a study of strategic interactions, including conflict and cooperation, between rational decision makers following some mathematical models. It has shown enormous successful applications in social, network, and computer sciences as well as engineering [1]–[5]. A cooperative game is a strategic situation where the players (i.e., decision makers) can make binding agreement to form coalitions. In contrast, the players in a non-cooperative game can make decisions independently to obtain their own best interests.

Differential game is usually cast into a non-cooperative game, where each player can influence the evolution of a state vector in a dynamical system modeling by differential equations; it is closely related to optimal control, but with two or more objective functions and control inputs. Players aim to reach their own objectives by designing their control inputs which then influence the common system. For differential game, two Nash equilibrium strategies, namely, open-loop and closed-loop Nash equilibria, are usually studied. Utilizing the information of current time and the initial state, open-loop strategies are developed for the case where the state vector is unknown [2], [3]. Closed-loop strategies are the decision rules conditioned on the current state and time information. Owing to exhibiting more robustness to disturbances in practical dynamical systems, more attention are focusing on closed-loop Nash equilibrium strategies [6]–[8]. Although game theory based control strategies have been used in intelligent transport for intersection traffic control [9], driver modeling [10], lane changing [11], [12], and cooperative merging [13], employing the idea of non-cooperative differential game for autonomous vehicles' simultaneous path tracking and lateral stabilization has not been well investigated in the existing literature.

A persistent tracking problem is investigated in [14] and a game-theoretic control strategy is designed for a mobile robot to keep the tracking distance within a detection range while tracking a moving target. Lane change decisions and control-level accelerations are evaluated in [13] for an automated driving control system, which has a receding horizon control scheme to determine discrete desired lane sequences. The problem is formulated as a differential game, in which the steering and acceleration control decisions are made based on the expected behaviour of other vehicles. A passive proactive lane change framework is presented in [12] through a combination of deep reinforcement learning and game theory for lane change scenarios. A target pursuit model for intelligent vehicles together with a motion planning scheme based on the Stackelberg differential game is presented in [15], in which terminal sliding mode approach is used to design a path tracking controller by active front steering. A cooperative difference game is used in [16] to develop a vehicle lateral stability controller, in which the players are the driver and direct yaw controller for a bicycle vehicle model that utilizes a linear pure-slip tire model. A path tracking control framework, in which a dynamic difference game is used for active front and rear steering actuation for tracking and vehicle lateral stabilization, is developed in [8].

Maintaining autonomous vehicles lateral stability during path tracking is challenging due to different control inputs, which might be conflicting based on various cost functions in the vehicle body control and wheel dynamic stabilization programs. This paper proposes a new game theory based framework for stability control and path tracking of automated driving systems, in which guidance and corner traction control strategies are formulated in terms of players in a differential game. The main contributions of this paper are: ***i)*** An integrated stability and path tracking control framework for automated driving are developed based on a non-cooperative differential game; and ***ii)*** The wheel dynamics and bidirectional slip effect, which reflect more accurate model description, are included in the framework to generate control inputs that are feasible. The reason for choosing a non-cooperative game is various stabilization, guidance, and traction control programs (by different manufacturers) that may not necessarily have access to the cost function of other decision makers. The remainder of the paper is

Ehsan Hashemi is with the Department of Mechanical and Mechatronics Engineering, University of Waterloo, Waterloo, ON, Canada (ehashemi@uwaterloo.ca). Xingkang He and Karl H. Johansson are with Division of Decision and Control Systems, School of Electrical Engineering and Computer Science. KTH Royal Institute of Technology, Sweden ((xingkang,kallej)@kth.se). Their work was supported by Knut & Alice Wallenberg Foundation, and Swedish Research Council.

organized as follows: Section II provides preliminaries and model description. The controller framework including the dynamical game for controller design is provided in Section III. The performance of the proposed non-cooperative differential game is investigated in Section IV through software simulations for (combined-slip) lane-change scenarios. The conclusion is drawn in Section V.

II. Preliminaries and Model Description

Tire forces are nonlinear functions of longitudinal and lateral slips, normal forces, and tire parameters. Due to complexities in such nonlinear bidirectional slip model, tire forces at each corner/tire ij, where $i \in \{f, r\}$ (front and rear axles) and $j \in \{l, r\}$ (left and right tires) are approximated by affine functions in this paper. Fig. 1a shows normalized lateral tire forces (by vertical forces), which change not only by slip ratio σ (horizontal axis), but by slip angle α (variations across the plots). A double-track vehicle model is used for the game theory based controller framework in this paper. In this model, the vehicle longitudinal speed, lateral speed, and yaw rate measured at vehicle CG are denoted by u, v, and $\dot{\theta}$, respectively; wheel speeds at each corner are ω_{ij}; and position and attitude tracking errors are denoted by $\varepsilon_y, \varepsilon_\theta$. The slip ratio is defined in terms of the longitudinal relative velocity as $\sigma_{ij} = \frac{\tilde{u}_{ij}}{h_{ij}}$, where $\tilde{u}_{ij} = R\omega_{ij} - u^t_{ij}$ is the relative longitudinal velocity at each tire due to the slip, R is the tire rolling radius, u^t_{ij} is the longitudinal speed in the tire coordinates that can be obtained by mapping vehicle's CG speed u to each corner, and $h_{ij} = R\omega_{ij}$ for the acceleration case ($\tilde{u}_{ij} \geq 0$) and $h_{ij} = u^t_{ij}$ for the brake case ($\tilde{u}_{ij} < 0$). The total slip angles (at each corner) are denoted by α_{ij} and are defined in terms of vehicle longitudinal/lateral states as

$$\alpha_{fj} = \delta_f + \beta_f, \ \alpha_{rj} = \beta_r, \tag{1}$$

in which we define $\beta_f := -\tan^{-1}\frac{v_f}{u_f}$ and $\beta_r := -\tan^{-1}\frac{v_r}{u_r}$, whereas $v_f = v + l_f\dot{\theta}$, $u_f = u + 0.5\kappa_j\dot{\theta}W_f$ and $v_r = v - l_r\dot{\theta}$, $u_r = u + 0.5\kappa_j\dot{\theta}W_r$. The distances from the center of the front and rear axles to CG are denoted by l_f, l_r, the front and rear track widths are W_f, W_r, and $\kappa_l = -\kappa_r = 1$.

For the vehicle stability and path following controllers in this paper, lateral tire forces are affinely described by $C^1_\alpha(\tilde{u}_{ij})\alpha_{ij}$ for $\forall|\alpha_{ij}| < \alpha_{st}$ or $-C^2_\alpha(\tilde{u}_{ij})\alpha_{ij} + d^2_{ij}$ for $\forall|\alpha_{ij}| \geq \alpha_{st}$, where α_{st} is the saturation slip angle shown by circles in Fig. 1a.

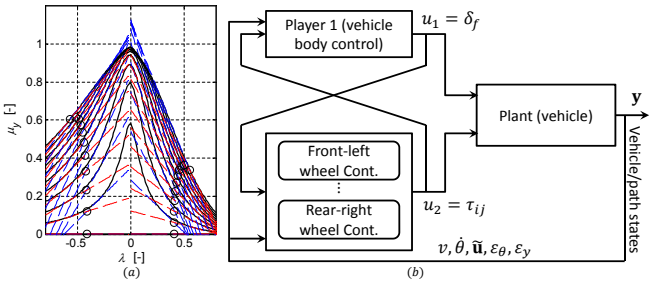

Fig. 1: (a) Normalized lateral forces (b) Game-theoretic realization for guidance control and stabilization

Normalized longitudinal forces at each tire also change with respect to the slip ratio σ_{ij} and the slip angle α_{ij} by considering the bidirectional slip effect. Similar to lateral forces, nonlinear longitudinal tire forces are affinely described by $C^1_\sigma(\alpha_{ij})\sigma_{ij}$ for $\forall|\sigma_{ij}| < \sigma_{st}$ or $-C^2_\sigma(\alpha_{ij})\sigma_{ij} + \bar{d}^2_{ij}$ for $\forall|\sigma_{ij}| \geq \sigma_{st}$, where σ_{st} is the saturation slip ratio. It should be mentioned that $C_\alpha(\tilde{u}_{ij})$ and $C_\sigma(\alpha_{ij})$ resembles dependency of cornering and longitudinal tire stiffness to longitudinal and lateral slips $\tilde{u}_{ij}, \alpha_{ij}$, respectively (bidirectional slip effect). Hence, the following general affine form is used as corner forces in the dynamic model description:

$$F_{y_{ij}} = C_\alpha(\tilde{u}_{ij})\alpha_{ij} + d_{ij}, \quad F_{x_{ij}} = C_\sigma(\alpha_{ij})\sigma_{ij} + \bar{d}_{ij} \tag{2}$$

By assuming longitudinal speed u as updated measurement at each time step in (1), the rate of β_{ij} at each corner yields

$$\dot{\beta}_{ij} = \tau^r_{ij}\dot{r} + \tau^v_{ij}\dot{v}, \tag{3}$$

in which τ^r_{ij} and τ^v_{ij} are provided for front and rear axles in Appendix I. The vehicle path following errors include the lateral distance component ε_y from the vehicle CG to its orthogonal projection point $\bar{o}$ on the center line of the desired path; and the heading error component $\varepsilon_\theta = \theta - \theta^r$, in which θ^r is the reference heading (tangential to the desired path). The tracking error dynamics can be written as follows by assuming small heading error [17]:

$$\dot{\varepsilon}_\theta = \dot{\theta} - u\varsigma, \quad \dot{\varepsilon}_y = u\varepsilon_\theta + v, \tag{4}$$

where ς is the curvature of the desired path at point $\bar{o}$.

Using vehicle lateral kinetics, we can express yaw acceleration and the rate of lateral speed as follows for the double-track vehicle model:

$$\ddot{\theta} = \frac{1}{I_z}[l_f F_{y_f}\mathrm{c}\delta - l_r F_{y_r} - \frac{W_f}{2}\tilde{F}_{y_f}\mathrm{s}\delta + \frac{W_r}{2}\tilde{F}_{x_r} + (\frac{W_f}{2}\mathrm{c}\delta + l_f\mathrm{s}\delta)F_{x_{fl}} + (-\frac{W_f}{2}\mathrm{c}\delta + l_f\mathrm{s}\delta_s)F_{x_{fr}}], \tag{5}$$

$$\dot{v} = \frac{1}{m}(F_{y_f}\mathrm{c}\delta + F_{y_r} + F_{x_f}\mathrm{s}\delta) - \dot{\theta}u, \tag{6}$$

where F_{x_f} is the total longitudinal force on the front axle; F_{y_f} and F_{y_r} are the total lateral forces on front and rear axles; and $\tilde{F}_{y_f} = F_{y_{fl}} - F_{y_{fr}}$ and $\tilde{F}_{x_r} = F_{x_{rl}} - F_{x_{rr}}$ are lateral and longitudinal force differences between the left- and right-side tires. We define $\mathrm{c}* = \cos(*)$ and $\mathrm{s}* = \sin(*)$ for simplicity. By using affine lateral force representation, the front and rear axle force components in the model can be expressed as

$$F_{y_f} = \beta_f(C_{\alpha_{fl}} + C_{\alpha_{fr}}) + \delta_f(C_{\alpha_{fl}} + C_{\alpha_{fr}}) + d_f, \tag{7}$$

$$F_{y_r} = \beta_r(C_{\alpha_{rl}} + C_{\alpha_{rr}}) + d_r, \tag{8}$$

$$\tilde{F}_{y_f} = \beta_f(C_{\alpha_{fl}} - C_{\alpha_{fr}}) + \delta_f(C_{\alpha_{fl}} - C_{\alpha_{fr}}) + \tilde{d}_f, \tag{9}$$

where $d_f = d_{fl} + d_{fr}, d_r = d_{rl} + d_{rr}, \tilde{d}_f = d_{fl} - d_{fr}$. For ease of notation, $C_\alpha(\tilde{u}_{ij})$ is replaced with $C_{\alpha_{ij}}$.

In addition to the lateral kinetics, the wheel dynamics is used in the model description. The relative longitudinal acceleration at each corner is $\dot{\tilde{u}}_{ij} = R\dot{\omega}_{ij} - \dot{u}_{t_{ij}}$, where $\dot{u}_{t_{ij}}$ and $\dot{\omega}_{ij}$ are the longitudinal acceleration in the tire coordinates and wheel rotational acceleration. They can be obtained from Inertial Measurement Unit (IMU) and wheel speed data, respectively. By employing longitudinal forces $F_{x_{ij}}$ from (2) in the wheel dynamics and replacing $\tilde{u}_{ij} = \sigma_{ij}h_{ij}$, the relative longitudinal velocity dynamics at each

vehicle corner yield

$$\dot{\tilde{u}}_{ij} = -\frac{R^2 C_{\sigma_{ij}}}{I_w h_{ij}} \tilde{u}_i j + \frac{R}{I_w} \tau_{ij} + h_{ij}^w, \tag{10}$$

where τ_{ij} is the total effective torque on each wheel; I_w is the wheels moment of inertia; and the term h_{ij}^w that includes mapped acceleration to corners and affine components, is provided in Appendix I. The tire model stiffness $C_\sigma(\alpha_{ij})$ is replaced by $C_{\sigma_{ij}}$ for ease of notation.

The state variable dynamics from (3) to (6) and longitudinal relative acceleration in (10) are used to develop the generalized system model description as

$$H\dot{\mathbf{x}}(t) = A\mathbf{x}(t) + B\mathbf{u}(t) + E\mathbf{h}(t), \tag{11}$$

with the output $\mathbf{y} = C\mathbf{x}$ where H, A, B, E, and C are provided in Appendix I. The inputs to the model are front steering by the automated driving system and the total torques applied at each tire, i.e., $\mathbf{u} = [\delta_f \ \tau_{fl} \ \tau_{fr} \ \tau_{rl} \ \tau_{rr}]^\top$. The state variables for the prediction model are vehicle lateral speed, yaw rate, modified corners' slip angle, relative longitudinal slip, and path following errors as $\mathbf{x} = [v \ \dot{\theta} \ \beta_f \ \beta_r \ \mathbf{v}_r \ \varepsilon_\theta \ \varepsilon_y]^\top$, in which $\tilde{\mathbf{u}} = [\tilde{u}_{fl} \ \tilde{u}_{fr} \ \tilde{u}_{rl} \ \tilde{u}_{rr}]^\top$. The $\mathbf{h}$ vector includes

$$\mathbf{h} = [h^v \ h^r \ h_{fl}^w \ h_{fr}^w \ h_{rl}^w \ h_{rr}^w \ u]^\top, \tag{12}$$

where h^v, h^r, and h_{ij}^w are provided in Appendix I. The outputs are the vehicle lateral speed, yaw rate, and path following errors as $\mathbf{y} = [v \ \ \dot{\theta} \ \ \varepsilon_\theta \ \ \varepsilon_y]^\top$. To deal with computational complexities for real-time implementation of this model and avoid conflicting inputs by different stabilization/path following programs, a game-theoretic approach is employed for designing a controller in the next section.

III. Controller Framework

The automated driving control system in this paper includes *i)* a vehicle body control strategy to stabilize the vehicle and minimize tracking errors, along with *ii)* wheel dynamic stabilization at each vehicle corner. These two types of controllers can be interpreted as two players in a dynamical game, which have no information about another player's cost function.

A. Game-Theoretic Approach

The control action of player 1 (vehicle body control) affects player 2 (thus, is an input to player 2 policy) and vice versa. This is schematically represented in Fig. 1b. In real vehicle stability control problem framework, **player 2** includes 4 players (at each vehicle corner), which is realized as components of player 2 in Fig. 1b. **Player 1**'s control objective is the vehicle lateral dynamic stabilization and path tracking described in (4) to (6); player 1 generates δ_f that alters α_{ij}, thus changes $F_{x_{ij}}$ and $C_{\sigma_{ij}}$ inside wheel dynamics (10) and affects player(s) 2 system. The relative longitudinal acceleration presented in (10) with the input τ_{ij} is used directly as the system for player 2. The control input τ_{ij}, applied by the player(s) 2 at each corner, evolve the states $\tilde{u}_{ij}$ in the wheel dynamics, thus will affect player 1's system dynamics (6) by changing the corner forces in (2).

The state variables and control inputs are rearranged for the two types of players in order to formally present the problem in a dynamical game framework. The state variables for player 1 are lateral speed (realized as body sideslip), yaw rate, front/rear axles' sideslip, and path tracking errors:

$$\mathbf{x}_1 = [v \ \dot{\theta} \ \beta_f \ \beta_r \ \varepsilon_\theta \ \varepsilon_y]^\top, \tag{13}$$

The control input from player 1 to the plant is the front steering, i.e. $\mathbf{u}_1 = \delta_f$. The outputs are the vehicle lateral responses, i.e. $\mathbf{y}_1 = [\dot{\theta} \ v]^\top$. The yaw rate $\dot{\theta}$ is a measured value by the vehicle control system's IMU. The lateral speed v can be measured by GPS or estimated as in [18], [19]. Player(s) 2 control actions are realized as corner brake torques:

$$u_2^1 = \tau_{fl}, \ u_2^2 = \tau_{fr}, \ u_2^3 = \tau_{rl}, \ u_2^4 = \tau_{rr} \tag{14}$$

Remark 1. *The objective for player(s) 2 is maintaining the relative longitudinal speed $\tilde{u}_{ij}$ (consequently slip ratio σ_{ij}) within a certain range, i.e. $|\tilde{u}_{ij}| \leq \sigma^b R\omega_{ij}$ for the acceleration ($\tilde{u}_{ij} \geq 0$) cases and $|\tilde{u}_{ij}| \leq \sigma^b u_{ij}^t$ for the brake ($\tilde{u}_{ij} < 0$) scenarios, where σ^b is a predefined bound.*

B. Dynamical Game Method for Controller Design

The integrated controller design problem is turned into a differential game problem in this part by assuming that the system matrices are time-invariant in a given time span (e.g., [0,T]). According to (11) and denoting $\bar{A} = H^{-1}A$, $\bar{B} = H^{-1}B$, $\bar{E} = H^{-1}E$, we have

$$\dot{\mathbf{x}}(t) = \bar{A}\mathbf{x}(t) + \bar{B}\mathbf{u}(t) + \bar{E}\mathbf{h}(t). \tag{15}$$

Suppose $\mathbf{x_d}$ is the constant desired state value, and $\tilde{\mathbf{x}}(t) = \mathbf{x}(t) - \mathbf{x_d}$ is the tracking error. Then we obtain the dynamics of the tracking error $\tilde{\mathbf{x}}(t)$ in the following

$$\dot{\tilde{\mathbf{x}}}(t) = \bar{A}\tilde{\mathbf{x}}(t) + \bar{B}\mathbf{u}(t) + f(t), \tag{16}$$

where $f(t) = \bar{E}\mathbf{h}(t) + \bar{A}\mathbf{x_d}$.

Let $\bar{B}_1 = H^{-1}B_1$, $\bar{B}_2 = H^{-1}B_2$, where B_1 and B_2 are given in Appendix. Then, we rewrite (16) with the following form

$$\begin{cases} \dot{\tilde{\mathbf{x}}}(t) = \bar{A}\tilde{\mathbf{x}}(t) + \bar{B}_1\mathbf{u_1}(t) + \bar{B}_2\mathbf{u_2}(t) + f(t) \\ \tilde{\mathbf{x}}(0) = \mathbf{x_0} - \mathbf{x_d}, \end{cases} \tag{17}$$

where $\mathbf{u_1}(t) = \delta_f$ is the control input by player 1, and $\mathbf{u_2}(t) = [\tau_{fl} \ \tau_{fr} \ \tau_{rl} \ \tau_{rr}]^\top$ is the control input by player 2.

For player i, $i \in \{1, 2\}$, the following linear-quadratic optimal control problem is considered

$$\mathbf{u_i^*}(\cdot) = \arg\min_{\mathbf{u_i}(\cdot)} J_i, \tag{18}$$

where

$$\begin{aligned} J_i = &\frac{1}{2}\tilde{\mathbf{x}}^\top(T) S_i \tilde{\mathbf{x}}(T) \\ &+ \frac{1}{2}\int_0^T \left\{\tilde{\mathbf{x}}^\top(t) Q_i(t) \tilde{\mathbf{x}}(t) + \mathbf{u_i}^\top(t) R_i(t) \mathbf{u_i}(t)\right\} dt \end{aligned} \tag{19}$$

subject to

$$\begin{cases} \dot{\tilde{\mathbf{x}}}(\mathbf{t}) = \bar{A}\tilde{\mathbf{x}}(t) + \bar{B}_i\mathbf{u_i}(t) + \bar{B}_j\mathbf{u_j^*}(t) + f(t), j \neq i \\ \tilde{\mathbf{x}}(0) = \mathbf{x_0} - \mathbf{x_d}, \end{cases} \tag{20}$$

where $S_i, Q_i(t)$ are positive semi-definite matrices, and $R_i(t)$ is a positive definite matrix, $0 \leq t \leq T$. Here, T is the terminal time.

According to [2], a 2-tuple of strategies $\{\mathbf{u_i^*}(t), i = 1, 2\}$ constitutes a Nash equilibrium solution if and only if for all

$\{\mathbf{u_i}(t), i = 1, 2\}$,

$$\begin{aligned} J_1^* &\triangleq J_1(\mathbf{u_1^*}(t), \mathbf{u_2^*}(t)) \leq J_1(\mathbf{u_1}(t), \mathbf{u_2^*}(t)) \\ J_2^* &\triangleq J_2(\mathbf{u_1^*}(t), \mathbf{u_2^*}(t)) \leq J_2(\mathbf{u_1^*}(t), \mathbf{u_2}(t)). \end{aligned} \tag{21}$$

According to [3] and [2], we provide the following two typical definitions on Nash equilibrium, namely, open-loop and closed-loop Nash equilibria.

Definition 1. *The 2-tuple $(\mathbf{u_1^*}(\cdot), \mathbf{u_2^*}(\cdot))$ is called an **open-loop (or a closed-loop) Nash equilibrium** if for each $i \in \{1, 2\}$, an optimal control path $\mathbf{u_i^*}(\cdot) = \phi_i(t)$ (or $\mathbf{u_i^*}(\cdot) = \varphi_i(\tilde{\mathbf{x}}(t), t)$) of the problem in* (18) *exists, where ϕ_i is a function of t (and $\varphi_i(\tilde{\mathbf{x}}(t), t)$ is a function of $\tilde{\mathbf{x}}(t)$ and t).*

In the following, we study the problems of how to obtain the open-loop Nash equilibrium and closed-loop Nash equilibrium, respectively, for the developed control system described by (17).

1) Open-loop Nash Equilibrium: For the differential game (18) – (20), the open-loop Nash equilibrium solution is given in the following theorem.

Theorem 1. *Suppose there exists a unique solution set $\{P_i(t)\}$ to* (22) *and a unique solution set $\{M_i(t)\}$ to* (23) *for each $i \in \{1, 2\}$.*

$$\begin{cases} \dot{P}_i(t) + P_i(t)\bar{A} + \bar{A}^T P_i(t) + Q_i(t) \\ \quad -P_i(t)\sum_{j=1}^{2} \bar{B}_j R_j^{-1}(t)\bar{B}_j^T P_j(t) = 0 \\ P_i(T) = S_i. \end{cases} \tag{22}$$

and

$$\begin{cases} \dot{M}_i(t) + \bar{A}^T M_i(t) + P_i(t)f(t) \\ \quad -P_i(t)\sum_{j=1}^{2} \bar{B}_j R_j^{-1}(t)\bar{B}_j^T M_j(t) = 0 \\ M_i(T) = 0. \end{cases} \tag{23}$$

Then, the differential game (18) – (20) *admits a unique open-loop Nash equilibrium solution given by*

$$\mathbf{u_i^*}(\mathbf{t}) = -R_i^{-1}(t)\bar{B}_i^T \left(P_i(t)\tilde{\mathbf{x}}^*(\mathbf{t}) + M_i(t)\right), \tag{24}$$

where $\tilde{\mathbf{x}}^*(\mathbf{t})$ is the associated state trajectory given in the following

$$\begin{aligned} \frac{d}{dt}\tilde{\mathbf{x}}^*(\mathbf{t}) &= \left(\bar{A} - \sum_{j=1}^{2} \bar{B}_j R_j^{-1}(t)\bar{B}_j^T P_j(t)\right)\tilde{\mathbf{x}}^*(\mathbf{t}) \\ &\quad - \sum_{j=1}^{2} \bar{B}_j R_j^{-1}(t)\bar{B}_j^T M_j(t) + f(t) \\ \tilde{\mathbf{x}}^*(\mathbf{0}) &= \mathbf{x_0} - \mathbf{x_d}. \end{aligned}$$

Proof: Define Hamiltonian function of players $i \in \{1, 2\}$ in the following

$$\begin{aligned} \mathcal{H}_i =& \tilde{\mathbf{x}}^{\mathbf{T}}(\mathbf{t})Q_i(t)\tilde{\mathbf{x}}(\mathbf{t}) + \mathbf{u_i^T}(\mathbf{t})R_i(t)\mathbf{u_i}(\mathbf{t}) \\ &+ \lambda_i^T(t)\left(\bar{A}\tilde{\mathbf{x}}(\mathbf{t}) + \bar{B}_1\mathbf{u_1}(\mathbf{t}) + \bar{B}_2\mathbf{u_2}(\mathbf{t}) + f(t)\right). \end{aligned}$$

According to the necessary condition for optimality [20], we have

$$\mathbf{u_i}(\mathbf{t}) = -R_i^{-1}(t)\bar{B}_i^T\lambda_i \tag{25}$$

$$\dot{\lambda}_i(t) = -Q_i(t)\tilde{\mathbf{x}}^{\mathbf{T}}(\mathbf{t}) - \bar{A}^T\lambda_i(t), \tag{26}$$

with the boundary condition $\lambda_i(T) = S_i\tilde{\mathbf{x}}(\mathbf{T})$. Taking (25) into (17) yields

$$\dot{\tilde{\mathbf{x}}}(\mathbf{t}) = \bar{A}\tilde{\mathbf{x}}(\mathbf{t}) - \sum_{i=1}^{2} \bar{B}_i R_i^{-1}(t)\bar{B}_i^T\lambda_i(t) + f(t). \tag{27}$$

Without losing generality, we suppose that $\lambda_i(t)$ has the form $\lambda_i(t) = P_i(t)\tilde{\mathbf{x}}(\mathbf{t}) + M_i(t)$. Because this assumption is trivially satisfied if $P_i(t) = 0$ and $\lambda_i(t) = M_i(t)$ for all t. Then taking the derivative of $\lambda_i(t)$ with respect to t, we have

$$\dot{\lambda}_i(t) = \dot{P}_i(t)\tilde{\mathbf{x}}(\mathbf{t}) + P_i(t)\dot{\tilde{\mathbf{x}}}(\mathbf{t}) + \dot{M}_i(t). \tag{28}$$

Submitting (26) and (27) into (28), we obtain an equation with the form $W_1(t)\tilde{\mathbf{x}}(\mathbf{t}) + W_1(t) = 0$. To guarantee this equation always satisfied, for all $t \in [0, T]$, we let $W_1(t) = 0$ and $W_2(t) = 0$. Thus we have the equations in (22) and (23), respectively. The boundary conditions are satisfied by noting that $\lambda_i(T) = S_i\tilde{\mathbf{x}}(\mathbf{T})$. The equation (24) is obtained by taking $\lambda_i(t) = P_i(t)\tilde{\mathbf{x}}(\mathbf{t}) + M_i(t)$ into (25) and (27).

2) Closed-loop Nash Equilibrium: For the differential game, the closed-loop Nash equilibrium solution is given in the following theorem.

Theorem 2. *Suppose there exists a unique solution set $\{Z_i(t)\}$ to* (29) *and there exists a unique solution set $\{N_i(t)\}$ to* (30) *for each $i \in \{1, 2\}$.*

$$\begin{cases} \dot{Z}_i(t) + Z_i(t)\bar{A} + \bar{A}^T Z_i(t) - \sum_{j=1}^{2} Z_i(t)\bar{B}_j R_j^{-1}(t)\bar{B}_j^T Z_j(t) \\ -\sum_{j=1}^{2} Z_j(t)\bar{B}_j R_j^{-1}(t)\bar{B}_j^T Z_i(t) \\ +Z_i(t)\bar{B}_i R_i^{-1}(t)\bar{B}_i^T Z_i(t) + Q_i(t) = 0, \\ Z_i(T) = S_i, \end{cases} \tag{29}$$

and

$$\begin{cases} \dot{N}_i(t) + \bar{A}^T N_i(t) + Z_i(t)f(t) \\ \quad +Z_i(t)\bar{B}_i R_i^{-1}(t)\bar{B}_i^T N_i(t) \\ \quad -\sum_{j=1}^{2} Z_i(t)\bar{B}_j R_j^{-1}(t)\bar{B}_j^T N_j(t) \\ \quad -\sum_{j=1}^{2} Z_j(t)\bar{B}_j R_j^{-1}(t)\bar{B}_j^T N_i(t) = 0 \\ N_i(T) = 0. \end{cases} \tag{30}$$

Then, the differential game (18) – (20) *admits a unique closed-loop Nash equilibrium solution given by*

$$\mathbf{u_i^*}(\mathbf{t}) = -R_i^{-1}(t)\bar{B}_i^T \left(Z_i(t)\tilde{\mathbf{x}}(\mathbf{t}) + N_i(t)\right). \tag{31}$$

Proof: According to the Hamilton–Jacobi–Bellman equation [20], we have

$$\begin{aligned} &\bigtriangledown_t V_i(t, x) \\ &= -\min_{\mathbf{u_i(t)}} \left\{ \bigtriangledown_x V_i(t, x) \left(\bar{A}\tilde{\mathbf{x}}(\mathbf{t}) + \sum_{j=1}^{2} \bar{B}_j\mathbf{u_j}(\mathbf{t}) + f(t)\right) \right. \\ &\quad \left. + \frac{1}{2}\tilde{\mathbf{x}}^{\mathbf{T}}(\mathbf{t})Q_i(t)\tilde{\mathbf{x}}(\mathbf{t}) + \frac{1}{2}\mathbf{u_i^T}(\mathbf{t})R_i(t)\mathbf{u_i}(\mathbf{t}) \right\}, \end{aligned} \tag{32}$$

where $V_i(t, x)$ is the cost function of player i from time t to the terminal time T, $\bigtriangledown_t V_i(t, x)$ is the partial derivative of $V_i(t, x)$ with respect to t, and $\bigtriangledown_x V_i(t, x)$ is the partial derivative of $V_i(t, x)$ with respect to x. By assuming that $V_i(t, x) = \frac{1}{2}\tilde{\mathbf{x}}^{\mathbf{T}}(\mathbf{t})Z_i(t)\tilde{\mathbf{x}}(\mathbf{t}) + N_i^T(t)\tilde{\mathbf{x}}(\mathbf{t}) + \Phi_i(t)$, we can obtain the control input

$$\mathbf{u_i}(\mathbf{t}) = -R_i^{-1}(t)\bar{B}_i^T \left(Z_i(t)\tilde{\mathbf{x}}(\mathbf{t}) + N_i(t)\right), \tag{33}$$

such that the right-hand side of (32) is achieved. Taking (33) and $\bigtriangledown_t V_i(t, x) = \frac{1}{2}\tilde{\mathbf{x}}^{\mathbf{T}}(\mathbf{t})\dot{Z}_i(t)\tilde{\mathbf{x}}(\mathbf{t}) + \dot{N}_i^T(t)\tilde{\mathbf{x}}(\mathbf{t}) + \dot{\Phi}_i(t)$ into

(32), we obtain

$$\tilde{\mathbf{x}}^{\mathbf{T}}(\mathbf{t})W_3(t)\tilde{\mathbf{x}}(\mathbf{t}) + p_1^T(t)(t)\tilde{\mathbf{x}}(\mathbf{t}) + p_2(t) = 0, \qquad (34)$$

where $W_3(t)$, $p_1(t)$ and $p_2(t)$ are appropriate time-varying matrices and vectors. (34) is satisfied if $W_3(t)+W_3^T(t) = 0$, $p_1(t) = 0$ and $p_2(t) = 0$. As a result, we obtain (29) and (30), respectively. Due to $V_i(T,x) = \frac{1}{2}\tilde{\mathbf{x}}^{\mathbf{T}}(\mathbf{T})S_i\tilde{\mathbf{x}}(\mathbf{T})$, comparing this with $V_i(T,x) = \frac{1}{2}\tilde{\mathbf{x}}^{\mathbf{T}}(\mathbf{T})Z_i(T)\tilde{\mathbf{x}}(\mathbf{T}) + N_i^T(T)\tilde{\mathbf{x}}(\mathbf{T}) + \Phi_i(T)$, we have $Z_i(T) = S_i$, $N_i(T) = 0$ and $\Phi_i(T) = 0$.

IV. Simulation Results

The proposed game-theoretic control strategy for autonomous vehicle path tracking and stability control is validated through simulations with an accurate model, which includes vehicle lateral dynamics and load transefr as well as a bidirectional slip force model that is identified by nonlinear least squares over the experimental tire force data form a Sedan vehicle with the model parameters $l_f = 135$ (cm), $l_r = 136$ (cm), $W_f = 155$ (cm), $W_r = 147$ (cm), $I_z = 4240$ (kg.m^2), $m = 1780$ (kg), $R = 33$ (cm), and $I_w = 1.4$ (kg.m^2). The simulations are performed based on the closed-loop Nash equilibrium solutions. A combined-slip lane-change maneuver (due to longitudinal slip by differential braking during cornering) with initial speed of 15 (m/s) is performed on a wet surface and the control actuation is brake modulation at all corners and active front steering. The steering control signals and vehicle lateral responses are compared in Fig. 2 for the proposed dynamic game based control strategy (DGC) and a model predictive controller (Cont.1), which is developed on system (11) with the prediction horizon of 8. Torque adjustments at each corner by

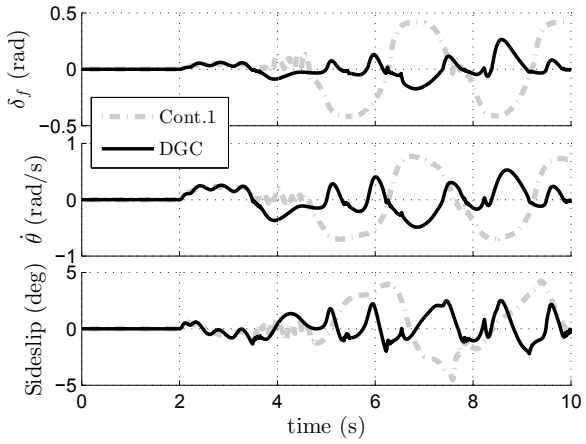

Fig. 2: Steering and vehicle lateral response in LC on wet

the dynamical game based and predictive control strategies are compared in Fig. 3. Both control strategies reduce lateral forces negative longitudinal slip (due to braking) and apply corrective yaw moment by brake and steering to track the desired path and at the same time avoid over-steer. However, the control actions for predictive strategy seem not cooperative in terms of minimizing tracking error and stabilizing the vehicle as can be seen from Fig. 2. This is due to the fact that the body and corner modules are not compromising; this leads to larger position and yaw tracking error as well as reduced speed due to longer brake involvement in Cont.1. Path tracking errors are also compared in Fig. 4, which shows

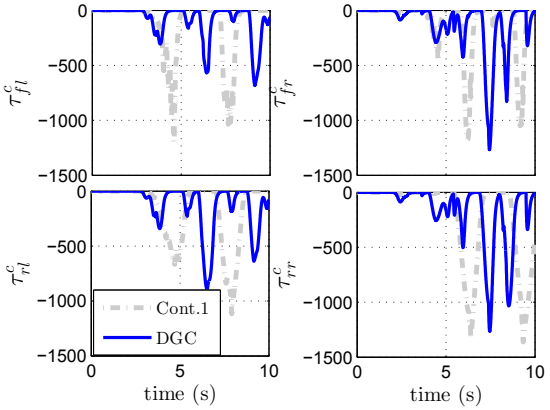

Fig. 3: Brake torque adjustments for the lane-change

better tracking performance for the proposed DGC and at the same time more stable lateral response (in Fig. 2) when compared with Cont.1

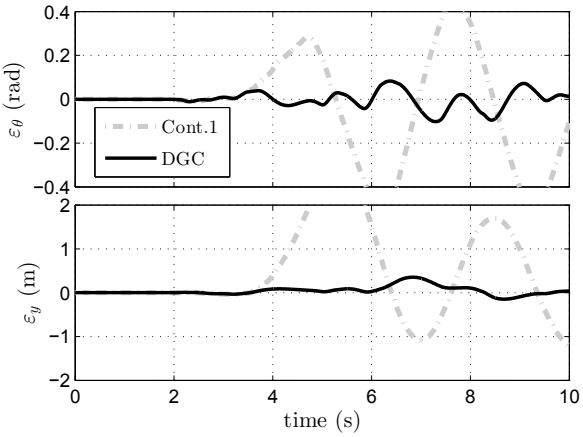

Fig. 4: Path tracking performance in LC on a slippery surface

V. Conclusion

This paper presented a new game theory-based control strategy with an integrated stabilization and guidance control framework for autonomous vehicles to resolve conflicts of control inputs that may arise during simultaneous yaw and path tracking as well as corner/wheel dynamic control. The lateral dynamic stabilization and path tracking tasks were formulated in a differential game, with braking at each corner and active front steering as control actuation. The open-loop and closed-loop Nash equilibrium control strategies were investigated by solving a two-player linear-quadratic differential game problem, respectively. This approach also allows for collaborative (such as cooperative adaptive cruise) control among various autonomous vehicles that may not necessarily have access to the model description and cost function of other vehicles in a shared driving environment. Simulations have been carried out for lane change maneuvers

on a slippery surface and confirmed that the developed controller improves tracking performance and enhances vehicle lateral stability effectively by compromising between two different control objectives in a dynamical game.

APPENDIX I
GENERALIZED MODEL COMPONENTS

The slip angle rate components in (3) are $\tau_{ij}^r = \frac{\partial \beta_{ij}}{\partial r}|_{\bar{r}}$ and $\tau_{ij}^v = \frac{\partial \beta_{ij}}{\partial v}|_{\bar{v}}$. These rates $\tau_{fj}^r = \frac{-l_f}{u\mathcal{K}_f}, \tau_{fj}^v = \frac{-1}{u\mathcal{K}_f}$ for the front axle and $\tau_{rj}^r = \frac{l_r}{u\mathcal{K}_r}, \tau_{rj}^v = \frac{-1}{u\mathcal{K}_r}$ for the rear axle, where $\mathcal{K}_f = 1 + (\frac{\bar{v}+l_f\bar{r}}{u})^2$ and $\mathcal{K}_r = 1 + (\frac{\bar{v}-l_r\bar{r}}{u})^2$. The operating point's (current) lateral and yaw speed are denoted by $\bar{v}$ and $\bar{r}$. The state, input, and output matrices in the generalized vehicle and wheel dynamics description (11) are

$$H = \left[\begin{array}{cccc|c} m & 0 & 0 & 0 & \\ 0 & I_z & 0 & 0 & \\ -\tau_f^v & -\tau_f^r & 1 & 0 & \mathbf{0}_{4\times 6} \\ -\tau_r^v & -\tau_r^r & 0 & 1 & \\ \hline \multicolumn{4}{c|}{\mathbf{0}_{6\times 4}} & \mathbf{I}_{6\times 6} \end{array}\right], \tag{A1}$$

$$A = \left[\begin{array}{cc|c|c} 0 & -mu & & \\ 0 & 0 & \mathscr{A}_1 & \mathbf{0}_{2\times 2} \\ \multicolumn{2}{c|}{\mathbf{0}_{6\times 2}} & \mathscr{A}_2 & \mathbf{0}_{6\times 2} \\ \hline 0 & 1 & & 0 \quad 0 \\ 1 & 0 & \mathbf{0}_{2\times 6} & u \quad 0 \end{array}\right], \tag{A2}$$

$$B = \begin{bmatrix} C_{\alpha_f} & 0 & 0 & 0 & 0 \\ l_f C_{\alpha_f} & 0 & 0 & 0 & 0 \\ & & \mathbf{0}_{2\times 5} & & \\ 0 & \frac{R}{I_w} & 0 & 0 & 0 \\ 0 & 0 & \frac{R}{I_w} & 0 & 0 \\ 0 & 0 & 0 & \frac{R}{I_w} & 0 \\ 0 & 0 & 0 & 0 & \frac{R}{I_w} \\ & & \mathbf{0}_{2\times 5} & & \end{bmatrix}, \tag{A3}$$

$$E = \left[\begin{array}{cc} \mathbf{I}_{2\times 2} & \mathbf{0}_{2\times 5} \\ \hline \multicolumn{2}{c}{\mathbf{0}_{2\times 7}} \\ \hline \mathbf{0}_{4\times 2} & \mathbf{I}_{4\times 4} \quad \mathbf{0}_{4\times 1} \\ \hline \mathbf{0}_{2\times 6} & -\kappa(\rho) \\ & 0 \end{array}\right], \; C = \left[\begin{array}{c|c} \mathbf{I}_{2\times 2} & \mathbf{0}_{2\times 8} \\ \hline \mathbf{0}_{2\times 8} & \mathbf{I}_{2\times 2} \end{array}\right], \tag{A4}$$

$$\mathscr{A}_1 = \begin{bmatrix} C_{\alpha_f} & C_{\alpha_r} & a_1^1 & a_1^2 & 0 & 0 \\ l_f C_{\alpha_f} & -l_r C_{\alpha_r} & a_1^3 & a_1^4 & a_1^5 & a_1^6 \end{bmatrix} \tag{A5}$$

$$\mathscr{A}_2 = \left[\begin{array}{c} \mathbf{0}_{2\times 6} \\ \hline \mathbf{0}_{4\times 2} \quad \frac{R}{I_w}\mathbf{I}_{4\times 4} \end{array}\right], \tag{A6}$$

where $C_{\alpha_f} = C_{\alpha_{fl}} + C_{\alpha_{fr}}$, $C_{\alpha_r} = C_{\alpha_{rl}} + C_{\alpha_{rr}}$, $a_1^1 = \frac{C_{\sigma_{fl}}\mathrm{s}\bar{\delta}}{h_{fl}}, a_1^2 = \frac{C_{\sigma_{fr}}\mathrm{s}\bar{\delta}}{h_{fr}}, a_1^3 = \frac{l_f C_{\sigma_{fl}}\mathrm{s}\bar{\delta}}{h_{fl}} + \frac{W_f C_{\sigma_{fl}}}{2h_{fl}}, a_1^4 = \frac{l_f C_{\sigma_{fr}}\mathrm{s}\bar{\delta}}{h_{fr}} - \frac{W_r C_{\sigma_{fr}}}{2h_{fr}}, a_1^5 = \frac{W_r C_{\sigma_{rl}}}{2h_{rl}}, a_1^6 = -\frac{W_r C_{\sigma_{rr}}}{2h_{rr}}$, and $\bar{\delta}$ is the measured steering angle in the previous time step. The components of uncontrolled input matrix $\mathbf{w}$ are $h^v = d_f + d_r + \bar{d}_f\mathrm{s}\bar{\delta}$, $h^r = l_f d_f - l_r d_r + l_f\bar{d}_f\mathrm{s}\bar{\delta} + \frac{W_f}{2}\tilde{d}_f + \frac{W_r}{2}\tilde{d}_r$, and $h_{ij}^w = -\dot{u}_{t_{ij}} - \frac{R^2}{I_w}\bar{d}_{ij}$, where $d_f = d_{fl} + d_{fr}, d_r = d_{rl} + d_{rr}, \bar{d}_f = \bar{d}_{fl} + \bar{d}_{fr}, \tilde{\bar{d}}_f = \bar{d}_{fl} - \bar{d}_{fr}$, and $\tilde{\bar{d}}_r = \bar{d}_{rl} - \bar{d}_{rr}$. d_{ij} and $\bar{d}_{ij}$ are the affine tire force components discussed in Section II. The input matrices introduced in the system (17) are:

$$B_1 = \begin{bmatrix} C_{\alpha_f} \\ l_f C_{\alpha_f} \\ \mathbf{0}_{8\times 1} \end{bmatrix}, \; B_2 = \begin{bmatrix} \mathbf{0}_{4\times 4} \\ \frac{R}{I_w}\mathbf{I}_{4\times 4} \\ \mathbf{0}_{2\times 4} \end{bmatrix}, \tag{A8}$$

REFERENCES

[1] G. Feichtinger and S. Jørgensen, "Differential game models in management science," *European Journal of Operational Research*, vol. 14, no. 2, pp. 137–155, 1983.

[2] T. Basar and G. J. Olsder, *Dynamic noncooperative game theory*. SIAM, 1999, vol. 23.

[3] E. J. Dockner, S. Jorgensen, N. Van Long, and G. Sorger, *Differential games in economics and management science*. Cambridge University Press, 2000.

[4] M. Eskelinen, "Towards computer game studies," *Digital creativity*, vol. 12, no. 3, pp. 175–183, 2001.

[5] S. Roy, C. Ellis, S. Shiva, D. Dasgupta, V. Shandilya, and Q. Wu, "A survey of game theory as applied to network security," in *2010 43rd Hawaii International Conference on System Sciences*. IEEE, 2010, pp. 1–10.

[6] D. Bauso, *Game theory with engineering applications*. SIAM, 2016.

[7] T. Mylvaganam, M. Sassano, and A. Astolfi, "A differential game approach to multi-agent collision avoidance," *IEEE Transactions on Automatic Control*, vol. 62, no. 8, pp. 4229–4235, 2017.

[8] X. Ji, Y. Liu, X. He, K. Yang, X. Na, C. Lv, and Y. Liu, "Interactive control paradigm-based robust lateral stability controller design for autonomous automobile path tracking with uncertain disturbance: A dynamic game approach," *IEEE Transactions on Vehicular Technology*, vol. 67, no. 8, pp. 6906–6920, 2018.

[9] M. O. Sayin, C.-W. Lin, S. Shiraishi, J. Shen, and T. Başar, "Information-driven autonomous intersection control via incentive compatible mechanisms," *IEEE Transactions on Intelligent Transportation Systems*, vol. 20, no. 3, pp. 912–924, 2018.

[10] N. Li, D. Oyler, M. Zhang, Y. Yildiz, A. Girard, and I. Kolmanovsky, "Hierarchical reasoning game theory based approach for evaluation and testing of autonomous vehicle control systems," in *2016 IEEE 55th Conference on Decision and Control (CDC)*. IEEE, 2016, pp. 727–733.

[11] H. Yu, H. E. Tseng, and R. Langari, "A human-like game theory-based controller for automatic lane changing," *Transportation Research Part C: Emerging Technologies*, vol. 88, pp. 140–158, 2018.

[12] G. Ding, S. Aghli, C. Heckman, and L. Chen, "Game-theoretic cooperative lane changing using data-driven models," in *2018 IEEE/RSJ International Conference on Intelligent Robots and Systems (IROS)*. IEEE, 2018, pp. 3640–3647.

[13] M. Wang, S. P. Hoogendoorn, W. Daamen, B. van Arem, and R. Happee, "Game theoretic approach for predictive lane-changing and car-following control," *Transportation Research Part C: Emerging Technologies*, vol. 58, pp. 73–92, 2015.

[14] M. Zhang and H. H. Liu, "Game-theoretical persistent tracking of a moving target using a unicycle-type mobile vehicle," *IEEE Transactions on Industrial Electronics*, vol. 61, no. 11, pp. 6222–6233, 2014.

[15] H. Wang, X. Yu, H. Song, Z. Lu, J. Lloret, and F. You, "A global optimal path planning and controller design algorithm for intelligent vehicles," *Mobile Networks and Applications*, vol. 23, no. 5, pp. 1165–1178, 2018.

[16] S. H. Tamaddoni, S. Taheri, and M. Ahmadian, "Optimal preview game theory approach to vehicle stability controller design," *Vehicle system dynamics*, vol. 49, no. 12, pp. 1967–1979, 2011.

[17] C. Hu, R. Wang, F. Yan, and N. Chen, "Robust composite nonlinear feedback path-following control for underactuated surface vessels with desired-heading amendment," *IEEE Transactions on Industrial Electronics*, vol. 63, no. 10, pp. 6386–6394, 2016.

[18] X. Zhang, Y. Xu, M. Pan, and F. Ren, "A vehicle ABS adaptive sliding-mode control algorithm based on the vehicle velocity estimation and tyre/road friction coefficient estimations," *Vehicle System Dynamics*, vol. 52, no. 4, pp. 475–503, 2014.

[19] E. Hashemi, M. Pirani, A. Khajepour, A. Kasaiezadeh, S.-K. Chen, and B. Litkouhi, "Corner-based estimation of tire forces and vehicle velocities robust to road conditions," *Control Engineering Practice*, vol. 61, pp. 28–40, 2017.

[20] D. E. Kirk, *Optimal control theory: an introduction*. Courier Corporation, 2012.